Implementation of Indirect Vector Control on an Integrated Digital Signal Processor - Based System

Mohammad N.Marwali Ali Keyhani, Senior Member WillyTjanaka, Student Member

Department of Electrical Engineering,
The Ohio State University,
Columbus, Ohio 43210

Abstract- This paper presents an implementation of indirect vector control of induction machine on an integrated DSP (Digital Signal Processor) system manufactured by dSPACE GmbH. The system integrates into a single board the computational power of a TMS320C31 DSP with extra peripherals needed in vector control application, and therefore requires minimal hardware development. The induction machine parameters required for the vector control operation are obtained through an off line parameters identification using Maximum Likelihood estimation technique with a DC voltage source excitation. It is shown through extensive experimental study that the off line identified parameters yield in a reliable field orientation of the induction machine.

Keywords : induction machine, vector control, parameter identification, modeling

LIST OF SYMBOLS

V_{ds}, V_{qs} : stator voltages in d-q stationary reference frame

i_{ds}, i_{qs} : stator currents in d-q stationary reference frame

i_{dr}, i_{qr} : rotor currents in d-q stationary reference frame

$\lambda_{ds}, \lambda_{qs}$: stator fluxes in d-q stationary reference frame

$\lambda_{dr}, \lambda_{qr}$: rotor fluxes in d-q stationary reference frame

V^e_{ds}, V^e_{qs} : stator voltages in d-q rotor-flux reference frame

i^e_{ds}, i^e_{qs} : stator currents in d-q rotor-flux reference frame

$\lambda^e_{ds}, \lambda^e_{qs}$: stator fluxes in d-q rotor-flux reference frame

PE-020-EC-0-2-1998 A paper recommended and approved by the IEEE Electric Machinery Committee of the IEEE Power Engineering Society for publication in the IEEE Transactions on Energy Conversion. Manuscript submitted April 16, 1997; made available for printing March 2, 1998.

$\lambda^e_{dr}, \lambda^e_{qr}$: rotor fluxes in d-q rotor-flux reference frame

ω_r : rotor mechanical speed (*rad/s*).

L_m : magnetizing inductance

L_{ls}, L_{lr} : stator and rotor leakage inductances

L_s, L_r : stator and rotor self inductances

R_s, R_r : stator and rotor resistances

J : rotor inertia constant ($kg \cdot m^2$)

B : damping coefficient ($N \cdot m \cdot s$)

T_L : load torque ($N \cdot m$)

T_e : produced electromagnetic torque ($N \cdot m$)

n_p : number of poles pairs

I. INTRODUCTION

Control of AC induction machines using the vector control techniques is becoming more popular nowadays. The need for extensive computations has no more become an objection to the vector control implementation. This is due to the wide availability of high speed digital processors. Digital signal processors with instruction cycle in the range of tens of nano-seconds are not uncommon these days [12].

In order to implement vector control of induction machine, certain interface peripherals must be specifically built in to the DSP system [7]. These peripherals include analog to digital converters for feedback signal acquisition, a set of timers for PWM generation, a speed encoder interface ,and digital to analog converters for signals tracing

The need to build such peripherals has previously increased the complexity and time required to implement a vector control system. Hence, availability of a single board that integrates all the peripherals would be of advantage. One such board is currently available from dSPACE GmbH. This board, which is based on the Texas Instrument TMS320C31 DSP contains all the peripherals mentioned above. It is one of the intention of

this paper, therefore, to describe the development of the indirect vector control using this type of system.

In order to implement a reliable vector control of induction machine, accurate machine parameters must be available. Many studies have been performed in off-line induction machine modeling and parameter estimation using steady state and transient test data. Recently, system identification techniques have been introduced to estimate the parameters of induction motor using standstill frequency response data and time domain response data [1].

In this paper, the linear parameters of an induction motor are identified from multiple sets of standstill time domain test data. The measurements used for the modeling are obtained by applying DC voltage source at the stator terminals while the machine is in standstill condition. The estimated parameters are validated by using standstill test, steady-state test, and dynamic test. However, only the results of dynamic test will be presented in this paper.

The induction machine parameters obtained from the off line parameter identification above are then used in the indirect vector control implementation. Various experimental study have been performed to verify the validity of the estimated parameters in vector control operation. The results are presented and analyzed in this paper.

II. VECTOR CONTROL OF INDUCTION MACHINE

Model of Induction Machine

Using the equivalent circuits of induction machine in d-q stationary reference frame as shown in Fig. 1, the following basic equations of induction machine can be derived [4].

$$V_{qs} = R_s i_{qs} + p\lambda_{qs} \tag{1.a}$$

$$V_{ds} = R_s i_{ds} + p\lambda_{ds} \tag{1.b}$$

$$0 = R_r i_{qr} - n_p \omega_r \lambda_{dr} + p\lambda_{qr} \tag{1.c}$$

$$0 = R_r i_{dr} + n_p \omega_r \lambda_{qr} + p\lambda_{dr} \tag{1.d}$$

The fluxes are given by :

$$\lambda_{qs} = (L_{ls} + L_m) i_{qs} + L_m i_{qr} = L_s i_{qs} + L_m i_{qr} \tag{2.a}$$

$$\lambda_{ds} = (L_{ls} + L_m) i_{ds} + L_m i_{dr} = L_s i_{ds} + L_m i_{dr} \tag{2.b}$$

$$\lambda_{qr} = (L_{lr} + L_m) i_{qr} + L_m i_{qs} = L_r i_{qr} + L_m i_{qs} \tag{2.c}$$

$$\lambda_{dr} = (L_{ls} + L_m) i_{dr} + L_m i_{ds} \tag{2.d}$$

with $L_s = L_{ls} + L_m$ and $L_r = L_{lr} + L_m$.

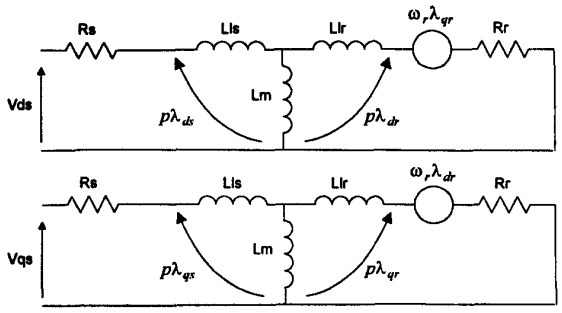

Fig. 1 Equivalent circuit in d-q stationary

Based on the d-q stationary reference model in (1) and (2), the state space model of induction machine in the stationary reference frame can be derived. Choosing the rotor speed (ω_r), stator currents (i_{qs}, i_{ds}), and rotor fluxes ($\lambda_{qr}, \lambda_{dr}$) as the state variables of the system , the following state space model (3.a)-(3.e) is obtained (see [5] and [6] for derivations).

$$\frac{d\omega_r}{dt} = \mu\left(\lambda_{dr} i_{qs} - \lambda_{qr} i_{ds}\right) - \frac{B}{J}\omega_r - \frac{T_L}{J} \tag{3. a}$$

$$\frac{d\lambda_{qr}}{dt} = n_p \omega_r \lambda_{dr} - \eta\lambda_{qr} + \eta L_m i_{qr} \tag{3..b}$$

$$\frac{d\lambda_{dr}}{dt} = -n_p \omega_r \lambda_{qr} - \eta\lambda_{dr} + \eta L_m i_{dr} \tag{3..c}$$

$$\frac{di_{qs}}{dt} = -\beta n_p \omega_r \lambda_{dr} + \eta\beta\lambda_{qr} - \gamma i_{qs} + \frac{1}{\sigma L_s} v_{qs} \tag{3.d}$$

$$\frac{di_{ds}}{dt} = \beta n_p \omega_r \lambda_{qr} + \eta\beta\lambda_{dr} - \gamma i_{ds} + \frac{1}{\sigma L_s} v_{ds} \tag{3.e}$$

with constants defined as follows :

$$\eta \equiv \frac{1}{T_R} = \frac{R_r}{L_r}, \quad \sigma \equiv 1 - \frac{L_m^2}{L_s L_r}, \quad \beta \equiv \frac{L_m}{\sigma L_s L_r},$$

$$\gamma \equiv \frac{L_m}{\sigma L_s L_r^2} + \frac{R_s}{\sigma L_s}, \quad \mu \equiv n_p \frac{L_m}{J L_r}$$

The electromagnetic torque expressed in terms of the state variables is :

$$T_e = \mu J\left(\lambda_{dr} i_{qs} - \lambda_{qr} i_{ds}\right) \tag{4}$$

Vector Control

The objective of vector control of induction machine is to allow an induction machine to be controlled just like a separately excited dc machine [3,4]. This is achieved through transformations of variables to a coordinate reference frame that rotates along with the rotor flux. Specifically, define

$$|\lambda_R| \equiv \sqrt{\lambda_{qr} + \lambda_{dr}} \qquad \theta_e \equiv \arctan\frac{\lambda_{qr}}{\lambda_{dr}} \tag{5}$$

as the magnitude and angle of the rotor flux. Then, the transformation of variables to the rotor flux reference frame is given by,

$$\begin{bmatrix} f_d^e \\ f_q^e \end{bmatrix} = \begin{bmatrix} \cos\theta_e & \sin\theta_e \\ -\sin\theta_e & \cos\theta_e \end{bmatrix} \begin{bmatrix} f_d \\ f_q \end{bmatrix} = \frac{1}{|\lambda_R|} \begin{bmatrix} \lambda_{dr} & \lambda_{qr} \\ -\lambda_{qr} & \lambda_{dr} \end{bmatrix} \begin{bmatrix} f_d \\ f_q \end{bmatrix} \tag{6}$$

Using definition (5) and applying transformation (6) to the rotor fluxes we have :

$$\lambda_{dr}^e = \sqrt{\lambda_{dr}^{\,2} + \lambda_{qr}^{\,2}} = |\lambda_r| = \lambda_r^e \tag{7.a}$$

$$\lambda_{qr}^e = 0 \tag{7.b}$$

Similar transformation can be applied to the d-q stator currents and a new state space model (8.a-8.e) can be derived with $\omega_r, \lambda_r^e, i_{qs}^e, i_{ds}^e, \theta_e$ as the transformed state variables [5, 6].

$$\frac{d\omega_r}{dt} = \mu \cdot \lambda_r^e \cdot i_{qs}^e - \frac{B}{J}\omega_r - \frac{T_L}{J} \tag{8.a}$$

$$\frac{d\lambda_r^e}{dt} = -\eta \cdot \lambda_r^e + \eta \cdot L_m \cdot i_{ds}^e \tag{8.b}$$

$$\frac{di_{qs}^e}{dt} = -\gamma \cdot i_{qs}^e - \beta n_p \omega_r \cdot \lambda_r^e - n_p \omega_r \cdot i_{ds}^e - \eta \cdot L_m \cdot \frac{i_{qs}^e \cdot i_{ds}^e}{\lambda_r^e} + \frac{1}{\sigma L_s} v_{qs}^e \tag{8.c}$$

$$\frac{di_{ds}^e}{dt} = -\gamma \cdot i_{ds}^e + \eta \cdot \beta \cdot \lambda_r^e + n_p \omega_r \cdot i_{qs}^e + \eta \cdot L_m \cdot \frac{i_{qs}^{e\,2}}{\lambda_{dr}^e} + \frac{1}{\sigma L_s} v_{qs}^e \tag{8.d}$$

$$\frac{d\theta_e}{dt} = n_p \omega_r + \eta L_m \frac{i_{qs}^e}{\lambda_r^e} \tag{8.e}$$

and the expression for torque is given by :

$$T_e = \mu J \cdot \lambda_r^e \cdot i_{qs}^e \tag{9}$$

If the induction machine is driven by a current source inverter then, from (8.b), it can be seen that the dynamics of rotor flux is linear and only dependent on the d-current input. Moreover, if the rotor flux can be kept at a constant value the rotor speed dynamics (8.a) becomes a linear system with the q-current as the input. PI controllers can be used [3, 4] to force the rotor flux and speed to follow the reference values as in :

$$i_{qs}^{e\,*} = K_{P1}\left(\omega_r^{\,*} - \omega_r\right) + K_{I1}\int\left(\omega_r^{\,*} - \omega_r\right)dt \tag{10}$$

$$i_{ds}^{e\,*} = K_{P2}\left(\lambda_r^{e\,*} - \lambda_r^e\right) + K_{I2}\int\left(\lambda_r^{e\,*} - \lambda_r^e\right)dt \tag{11}$$

where the starred variables represent the commanded (reference) values of the variables.

The output of the PI controllers must be limited in order not to exceed the current rating of the motor and drive system. In this case variable current limiter suggested by [8] can be used. Fig. 2 shows a block diagram of the variable current limiter. Note, however that Fig. 2 differs than that of [8] since the priority is given to the q-current command.

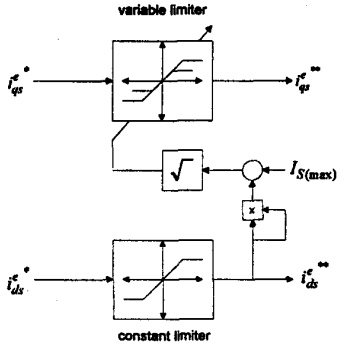

Fig. 2. Variable current limiter

Indirect Vector Control

In the indirect vector control, the unit vectors $(\sin\theta_e, \cos\theta_e)$ are computed by calculating the rotor flux angle θ_e from equation (8.e). Specifically define the synchronous frequency, ω_e, then obviously (since rotor flux rotates at synchronous frequency)

$$\omega_e = d\theta_e / dt \tag{12}$$

The slip angle can be expressed as :

$$\omega_{sl} = \omega_e - n_p\omega_r = \eta L_m \frac{i_{qs}^e}{\lambda_r^e} = \frac{L_m}{T_R}\frac{i_{qs}^e}{\lambda_r^e} \tag{13}$$

From (8.e) ,(12), and (13) we have :

$$\theta_e = \int \omega_e dt = \int\left(n_p\omega_r + \omega_{sl}\right)dt \tag{14}$$

The rotor flux can be estimated by solving for the rotor flux in (8.b) i.e.

$$\lambda_r^e = \frac{L_m}{T_R s + 1} i_{ds}^e \tag{15}$$

Fig. 3 shows a block diagram of the complete indirect vector control. In Fig. 3, the rotor flux angle θ_e is computed recursively using the actual d-q currents in the rotor flux reference frame. This approach should be contrasted with the feed-forward indirect vector control in [4] where the rotor flux angle is computed from the commanded d-q currents. Two PI controllers with limiters are used to control the speed and rotor flux as explained in the previous section. These two PI controllers yield the commanded d-q currents in the rotor flux reference frame.

PI current controllers with decoupling compensation, which will be explained in the next section, have been incorporated to control the stator currents to follow the commanded currents. Finally, a space vector PWM is used to produce the instantaneous generation of the commanded stator voltages.

Current Controller and Decoupling Compensation [8]

If a voltage source PWM inverter is used, the stator currents need to be controlled to track the commanded (reference) currents. As can be seen from (8.c) and (8.d), the dynamics of stator currents with stator voltages as inputs are coupled and non-linear. However if the stator voltages commands are given in the form of

$$v_{qs}^{e\,*} = u_1 - v_{qs\_comp} \tag{16}$$

$$v_{ds}^{e\,*} = u_2 - v_{ds\_comp} \tag{17}$$

where

$$v_{qs\_comp} = \sigma L_s\left(-\beta\omega_r\lambda_r^e - n_p\omega_r\cdot i_{ds}^e - \eta\cdot L_m\cdot\frac{i_{ds}^e i_{qs}^e}{\lambda_r^e}\right)$$

$$= -\frac{L_m}{L_r}n_p\omega_r\lambda_r^e - \sigma L_s\omega_e i_{ds}^e \tag{18}$$

$$v_{ds\_comp} = \sigma L_s\left(n_p\omega_r\cdot i_{qs}^e + \eta\cdot L_m\cdot\frac{i_{qs}^{e\,2}}{\lambda_{dr}^e}\right) = \sigma L_s\omega_e i_{qs}^e \tag{19}$$

then the stator current dynamics reduce to

$$\frac{di_{qs}^e}{dt} = -\gamma\cdot i_{qs}^e + u_1 \tag{20.a}$$

$$\frac{di_{ds}^e}{dt} = -\gamma\cdot i_{ds}^e + \eta\cdot\beta\cdot\lambda_r^e + u_2 \tag{20.b}$$

Since the current dynamics in (20) are linear and decoupled, PI controllers can be used for current tracking i.e

$$u_1 = K_{P1}\left(i_{qs}^{e\,**} - i_{qs}^e\right) + K_{I1}\int\left(i_{qs}^{e\,**} - i_{qs}^e\right)dt \tag{21}$$

$$u_2^* = K_{P2}\left(i_{ds}^{e\,**} - i_{ds}^e\right) + K_{I2}\int\left(i_{ds}^{e\,**} - i_{ds}^e\right)dt \tag{22}$$

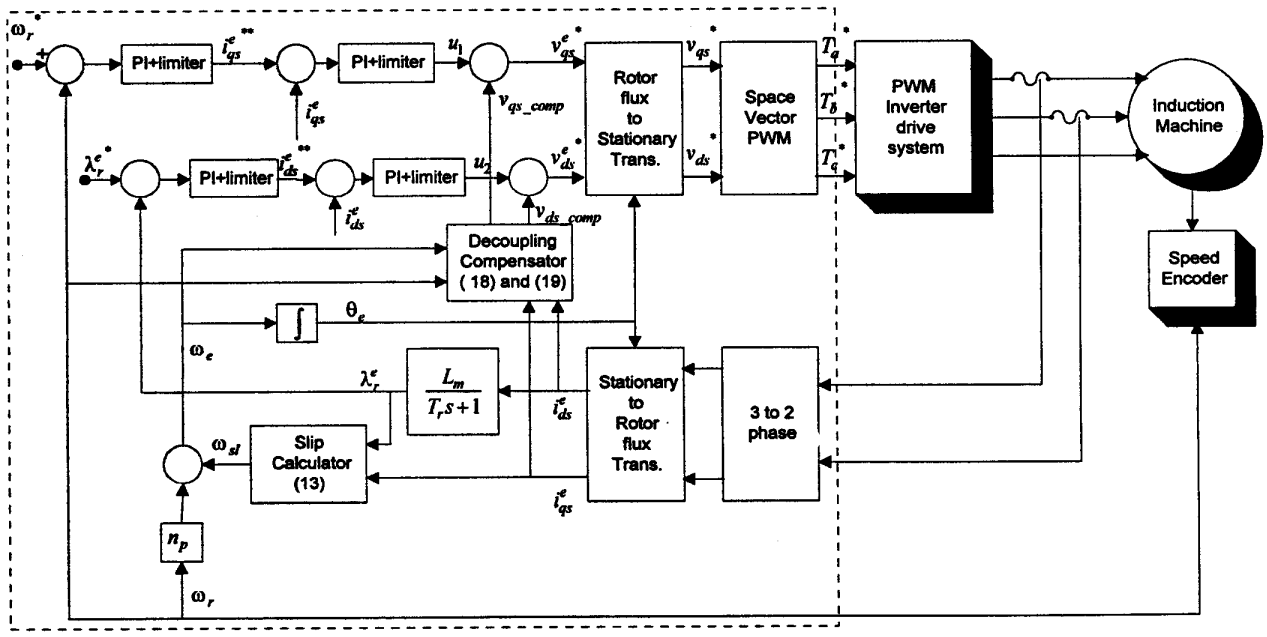

Fig.3 Indirect Vector Control

III OFF-LINE PARAMETER ESTIMATION

Maximum likelihood estimation method as outlined in [1, 2] is used to the estimate the induction machine parameters at stand still. This method has been known to yield in superior results for stand still parameter estimations in the presence of noise [1]. The block diagram of the identification process is shown in Fig. 4.

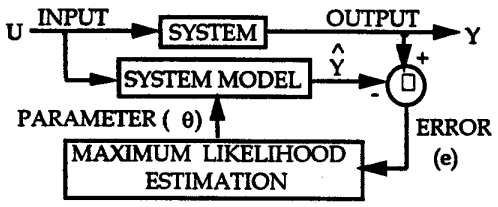

Fig. 4. Maximum likelihood estimation.

Identification Model

Under standstill condition, the q-axis equivalent circuit model in Fig. 1 reduces to that of Fig. 5 which represents a stand still second order model of induction machine. Due to symmetry of the rotor, the d-axis equivalent circuit model is identical to the q-axis model. Therefore, only q-axis model needs to be identified.

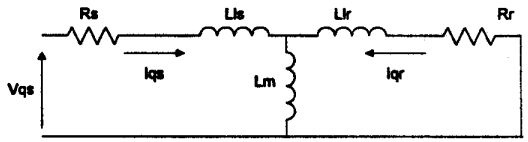

Fig. 5. Standstill 2nd order q-axis model of induction motor.

The dynamic equation of the second order model can be expressed as

$$\begin{bmatrix} V_{qs} \\ 0 \end{bmatrix} = \begin{bmatrix} R_s & 0 \\ 0 & R_r \end{bmatrix} \begin{bmatrix} I_{qs} \\ I_{qr} \end{bmatrix} + \begin{bmatrix} L_m + L_{ls} & L_m \\ L_m & L_m + L_{lr} \end{bmatrix} \cdot \frac{d}{dt} \begin{bmatrix} I_{qs} \\ I_{qr} \end{bmatrix} \quad (23)$$

Equation (23) can be reformulated as discrete-time state space equation given as [1]

$$X(k+1) = A(\theta) \cdot X(k) + B(\theta) \cdot U(k) + \omega(k) \quad (24.a)$$

$$Y(k+1) = C \cdot X(k+1) + \upsilon(k+1) \quad (24.b)$$

where $\omega(\cdot)$ and $\upsilon(\cdot)$ denote the process and measurement noise, respectively. For the second order model, the state, input, and output vectors are given as

$$X = \begin{bmatrix} I_{qs} & I_{qr} \end{bmatrix}^T \quad (25)$$

$$U = \begin{bmatrix} V_{qs} & 0 \end{bmatrix}^T \quad (26)$$

$$Y = \begin{bmatrix} I_{qs} \end{bmatrix} \quad (27)$$

$$C = \begin{bmatrix} 1 & 0 \end{bmatrix} \quad (28)$$

The parameter vector θ is

$$\theta = \begin{bmatrix} R_s & R_r & L_{ls} & L_m & L_{lr} \end{bmatrix} \quad (29)$$

In this study, since the voltage is the input and the current is the output, the transfer function $H(s)$ is expressed as the terminal admittance function [1].

$$H(s) = \frac{I_{qs}(s)}{V_{qs}(s)} = \frac{1}{Z_{qs}(s)} \quad (30)$$

Testing Procedure

The standstill time domain test configuration is shown in Fig. 6. Since the rotor of the induction motor is electrically symmetrical, the rotor position can be selected arbitrarily. The test data is recorded in terms of stator current and voltage. The DC voltage source Vb in Fig. 6 is a 24 VDC source, formed by connecting in series two deep cycle battery, each rated at 12 VDC and 700 A surge current. A variable resistor R1 is used to limit the current Is which flows into the motor stator windings. The steady state current is limited to 50% of peak rated current to prevent winding saturation. When switch S is closed, a step voltage input is applied across phase a and b of the terminals, and the data acquisition system is triggered simultaneously to record the data. The sampling rate is selected as 30 kHz and 16000 data points are acquired for each data set. The measurement errors are within ±1 %. Then, all the terminal voltages and currents are converted into stationary reference frame quantities by using the following equations :

$$V_{qs} = \frac{1}{2} V_s \quad (31)$$

$$I_{qs} = I_s \quad (32)$$

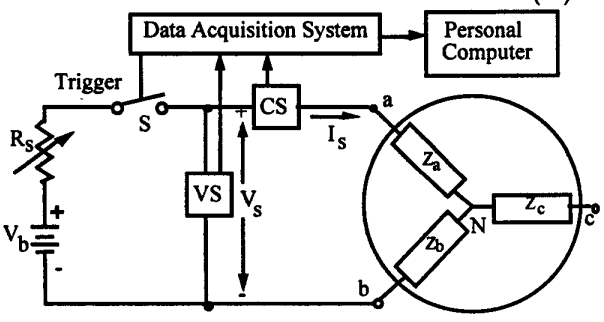

Fig. 6. Standstill time domain test configuration.

IV. DSP SYSTEM IMPLEMENTATION

The DSP system used for the vector control implementation is based on the DS1102 controller board from dSPACE GmbH. The heart of the DS1102 controller board is a Texas Instrument TMS320C31 32 bit DSP floating-point processor with 50 ns instruction cycle and

offers speed up to 40 million floating point operations per second (MFLOPS). The DS1102 is also equipped with a TI TMS320P14 16 bit Microcontroller-DSP that acts as a slave processor and provides the necessary digital I/O ports and powerful timer functions such as input capture, output compare, and PWM generation. Four channel Analog-to-Digital Converter (two 16 bit and two 12 bit) with integrated sample/hold circuits, four channel 16 bit DAC, and two incremental encoder interface are also available on the DS1102 board [11].

Fig. 7 shows the complete DSP system setup used for the vector control implementation. All the subsystems inside the dashed box in Fig. 3 are implemented inside the DS1102 controller board. The system requires only minimal external interface peripherals. Two machine terminal currents are sensed using current sensors and interfaced to the controller board built in A/D converter through a simple signal conditioner circuit. A 1024 pulse/revolution incremental optical encoder used for speed measurement can be safely interfaced to the DS1102 built- in encoder interface without requiring additional hardware.

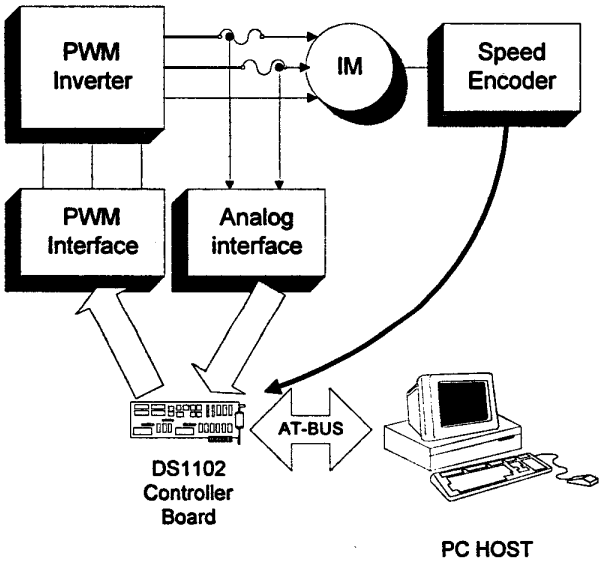

Fig. 7 DSP system setup

As depicted in Fig. 3, the space vector PWM algorithm described in [9] is used to produce the instantaneous stator command voltages. In this case, the on-chip PWM timers of the slave-DSP on the DS1102 provides the necessary gate timing, requiring only some simple external logic gates [10].

Control Software

The control software uses multiple update rate program similar to that of [7]. It uses the moving average filter to minimize the noise in the measured signals. In this case, a timer interrupt service routine is setup to read the values of terminal currents every 40 μsec and to perform a fifth order moving average filtering. The rotor flux magnitude and angle calculations, current controllers, and space vector PWM calculation are performed every five timer service routine i.e every 200 μsec. The slowest program update rate is applied to the speed and flux controllers calculations. These routines are executed every 1 ms intervals.

V. RESULTS AND DISCUSSION

A 3-phase, 4-pole, 1690 rpm, 2.5 hp, 220V/7A induction motor is used in this study. Parameters of the machine are identified using the previously outlined estimation method. Table 1 lists the estimated induction machine parameters.

TABLE 1
INDUCTION MOTOR PARAMETERS.

Parameters	Values
R_s (Ω)	0.28539
L_{ls} (mH)	1.8605
L_m (mH)	62.289
R_r (Ω)	0.79598
L_{lr} (mH)	2.9873

The identified model is validated by using standstill test, steady state test, and dynamic test [1,2]. However, only the results from dynamic test are presented here as shown in Fig. 8. As can be observed, the identified model is a reasonably accurate model. Note that the q-axis current has a larger error than the d axis -current. This is most probably due to some unmodeled structural dynamics or non-linear effects not included in the model used. This discrepancy, however, did not seem to affect the performance of the vector controlled machine.

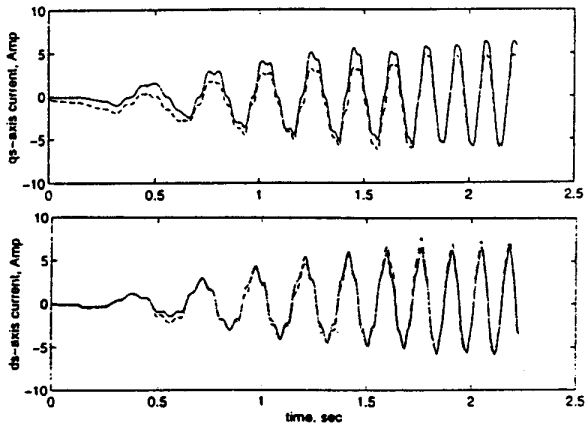

Fig. 8. Dynamic test for model validation : (a) qs-axis current (b) ds-axis currents. (__ experimental, — simulated)

The acquired parameters are then used for the implementation of the indirect vector control on the DSP system. Several experiments are conducted to test the validity of the estimated parameters in the indirect vector control operation. Some of the results are shown in Fig. 9 and Fig. 10.

In Fig. 9, the system is given a step reference speed of 1000 rpm. From Fig. 9.a, it can be seen that the steady state error of the speed is negligible, indicating a good speed tracking performance of the system. Fig. 9.b shows the estimated rotor flux being controlled to a constant value equal to the rated flux of 0.26 Wb/m2. As explained before, the constant rotor flux magnitude guarantees the linear relationship between the speed and q-current component in the rotor flux reference frame. Fig. 9.c and 9.d show the transient responses of the q-current in rotor flux and stationary reference frame respectively. In this case the maximum stator current is set to 10 A. The shapes of the q-current transient responses in Fig. 9.c and Fig. 9.d verify the proper field orientation of the induction machine [3].

Fig. 10 shows the experimental results when the machine is subjected to speed reversal operation. The reference speed in this case is a square-wave with 500 rpm amplitude and 5 sec period. Fig. 10.a displays the speed response showing that the system tracks the reference speed reasonably well. The proper operation of the current controller is verified by plotting the commanded and actual q-current in rotor reference frame as shown in Fig. 10.b and Fig. 10.c respectively. From these two figures, it can be seen that the actual current is able to follow the desired commanded current almost instantaneously. The actual stator current i_a ($=i_{qs}$) shown in Fig. 10.d can be seen to be confined to the 10 A limit.

VI. CONCLUSIONS

It is shown in this paper that a dedicated controller board that integrates the computing power of Digital Signal Processor and the necessary interface peripherals can substantially reduce the complexity and time required for the development of a vector control of induction machine. It is also shown through some experimental study that the off-line parameter estimation method used in this paper provides a reliable operation of the vector control system

VII. ACKNOWLEDGMENTS

This work is supported by the Center for Automotive Research (CAR) at the Ohio State University and Delphi Automotive System

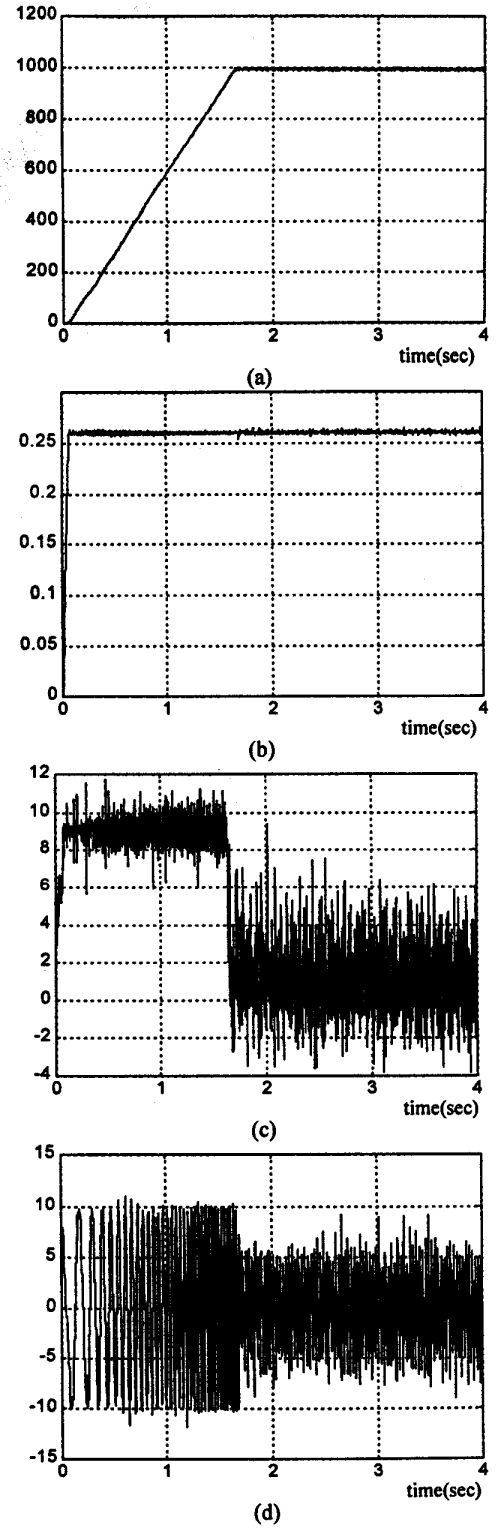

Fig. 9 : Speed reference 1000 rpm
(a) Rotor speed (rpm) (b) Rotor flux (Wb/m2)
(c) i_{qs}^{e} (A) (d) i_{qs} (A)

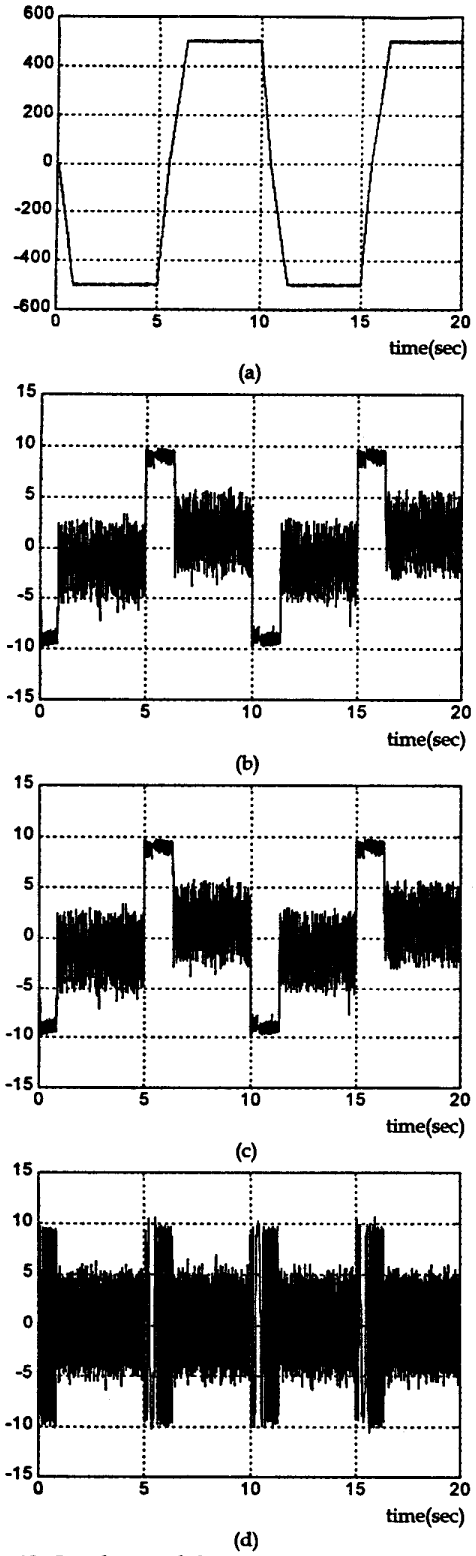

Fig. 10 : Speed reversal -500 rpm to 500 rpm
(a) Rotor speed (rpm) (b) i_{qs}^{e**} (A)
(c) i_{qs}^{e} (A) (d) i_{qs} (A)

VIII. REFERENCES

1. S. I. Moon and A. Keyhani, "Estimation of Induction Machine Parameters from Standstill Time Domain Data,", IEEE Trans. on Industrial Applications, Vol. 30, No. 6, Nov/Dec 1994
2. K. Astrom, "Maximum Likelihood and Prediction Error Methods," Automatica, vol. 16, pp. 551-574, 1980.
3. W. Leonard, Control of Electrical Drives, Springer, Berlin, Heidelberg, 1985
4. B. K. Bose, Power Electronics and AC Drives, Prentice Hall, 1986.
5. R. Marino, S Peresada, and P. Valigi, "Adaptive Input-Output Linearizing Control of Induction Motors" , IEEE Trans. on Automatic Control, Vol. 38, pp. 208-220, No. 2, Feb 1993
6. M. Bodson, J. N. Chiasson, R. T. Novotnak, "A Systematic Approach to Selecting Flux References for Torque Maximization in Induction Motors", IEEE Trans. on Control System Tech. Vol. 3, No. 4, pp 388-397, 1995
7. Xingyi Xu and Donald W. Novotny, "Implementation of Direct Stator Flux Orientation Control on a Versatile DSP Based System," IEEE Trans. on Industry Applications, vol. 27, no. 4, July/August 1991.
8. M. Koyama, M. Yano, I. Kamiyama, and S. Yano, "Microprocessor-Based Vector Control System for Induction Motor Drives with Rotor Time Constant Identification Function", IEEE Trans. on Industry Applications, Vol. IA-22, No.3, May/June 1986.
9. H. W. Van der Broeck and R.J. Kerkman, "Analysis and Realization of a pulse-width modulator based on voltage space vector", IEEE Trans. on Industry Applications, vol. 24, pp. 142-150, Jan./Feb 1988
10. Squirrel cage induction motor control with DS1102, Application Note, dSPACE GmbH, 1994
11. DS1102 User's Guide Version 2.0. dSPACE GmbH.
12. Digital Signal Processing Solutions Selection Guides, Texas Instrument, 1996

IX. BIOGRAPHIES

Mohammad N. Marwali received the B.S.E.E. degree from Institut Teknologi Bandung, Indonesia in 1993. From 1995 to 1997, he has been a graduate research associate at the Ohio State University. He received his M.S. degree from the Ohio State University in 1996. Currently, he is a Ph.D. candidate in electrical engineering at the Department of Electrical Engineering, Ohio State University.

Ali Keyhani received the Ph.D. degree from Purdue University, West Lafayette, Indiana in 1975. From 1967 to 1969, he worked for Hewlett-Packard Co. on the computer aided design of electronic transformers. Currently, he is a Professor of Electrical Engineering at the Ohio State University, Columbus, Ohio. His research interest is in control and modeling, parameter estimation, failure detection of electric machines, transformers, and drive systems.

Willy Tjanaka was born in Medan, North Sumatra, Indonesia, on October 4, 1971. He received the B.S.E.E. and M.S degree from the Ohio State University in 1994 and 1995 respectively. Currently, he is a design engineer at Philip Semiconductor